

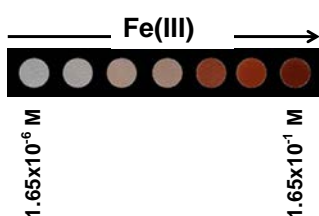
## Colorimetric detection, quantification and extraction of Fe(III) in water by acrylic polymers with pendant Kojic acid motifs

Saúl Vallejos,<sup>1</sup> Asunción Muñoz,<sup>1</sup> Félix Clemente García<sup>1</sup>, Roberta Colleoni,<sup>2</sup> Raffaella Biesuz,<sup>2</sup> Giancarla Alberti,<sup>2,\*</sup> José Miguel García<sup>1,\*</sup>

<sup>1</sup> Departamento de Química, Facultad de Ciencias, Universidad de Burgos, Plaza de Misael Bañuelos s/n, 09001 Burgos, Spain. Fax: (+) 34 947 258 831, Tel: (+) 34 947 258 085. E-mail: jmiguel@ubu.es

<sup>2</sup> Dipartimento di Chimica, Università di Pavia, via Taramelli 12, 27100 Pavia, Italy. Tel: (+) 39 0382 987347. E-mail: galberti@unipv.it

### Graphical abstract



### Research highlights

- A colorimetric sensory polymer for the detection of Fe(III) was synthesized.
- This polymer was prepared from a monomer derived from Kojic acid, which is a natural product.
- The film-shaped polymer was cut to obtain manageable solid sensory kits.
- Fe(III) was efficiently extracted, detected, discriminated and quantified from water.
- UV/vis and computer vision-based techniques were used for Fe(III) analysis.

### ABSTRACT

We synthesized a solid sensory material for the extraction, detection and quantification of iron(III) in aqueous media. The material is a film-shaped colorless polymer membrane that exhibits gel behavior. The Fe(III) extraction and sensing characteristics

are imparted by a new monomer derived from a natural product (i.e., Kojic acid), which exhibits chelating properties toward Fe(III). The sorption of Fe(III) on the membrane in water has been thoroughly characterized, including the sorption kinetics, sorption isotherms and profiles as a function of the pH. Fe(III) sorption followed pseudo first-order kinetics and required approximately 30 min to reach equilibrium. The maximum sorption capacity was approximately 0.04 mmol/g, and the sorption isotherms are well modeled by the Langmuir equation. The complexes that were found in the solid phase are in good agreement with those previously identified in the aqueous phase. Moreover, the sorption is highly specific (i.e., a recognition process) and results from the formation of a colored complex (iron(III)-Kojic acid derivative moieties). Therefore, the colorless sensory membrane turns red upon immersion in aqueous solutions containing Fe(III). The color output allows for both the qualitative visual determination of the Fe(III) concentration as well as also titration of Fe(III) using a) a UV/vis technique (limit of detection of  $3.6 \times 10^{-5}$  M; dynamic range of five decades, lower concentration =  $1.65 \times 10^{-6}$  M) and b) a computer vision-based analytical chemistry approach via color definition of the sensory membrane (RGB parameters) obtained from an image recorded with a handy device (e.g., a smartphone) (limit of detection of  $2.0 \times 10^{-5}$  M).

## **Keywords**

Sensory polymers, Kojic acid, visual detection, iron detection, iron extraction

## **1. INTRODUCTION**

The wide distribution of iron as cations in different oxidation states in the environment has both natural and anthropogenic origins. The latter is caused by its multiple applications in agriculture, industry, construction, medicine, households, and advanced

technological fields, which has led to increasing concerns over the potential effects of iron on the environment as well as in living things [1].

Therefore, the detection and quantification of iron salts is a fundamental task in chemistry due to its crucial role in living organisms and being extremely dangerous when its concentration exceeds a critical level. Its quantification is still a fundamental task in clinical chemistry but it is also of interest in environmental and agri-food fields. Currently, routine analyses are performed using methods that require trained staff and expensive equipment and techniques, such as atomic absorption spectroscopy (AAS) or inductively coupled plasma mass spectrometry (ICP-MS). However, chemical sensors allow for conversion of the iron salt concentration into signals that can be read by widely available instruments or even by an untrained observer, especially if the signal is a color change (chromogenic sensor). A sensor is a self-contained analytical device that is able to convert a physical quantity, which is related to a chemical species concentration, into a signal that can be read by an observer or an instrument [2-8]. Sensors are used in everyday objects and have innumerable applications that are often overlooked [9].

In recent years, we have focused on investigating solid-phase sensors for iron(III) analysis to develop a quick, easy and cheap method for the quantitative determination of metal ions [10-13]. In this study, we report a novel polymeric membrane for visual iron(III) sensing that features a derivative of Kojic acid as the receptor moiety. Kojic acid, which is a  $\gamma$ -pyrone derivative (5-hydroxy-2-(hydroxymethyl)-4-pyrone), is a natural heterocyclic chelating ligand [14], and anions of Kojic acid and its derivatives act as bidentate ligands to strongly coordinate to iron(III) via carbonyl and phenolic hydroxyl groups [15].

The film-shaped membrane is a manageable material that can be cut into solid sensory kits (e.g., small sensory discs). To develop a solid-phase sensor, the sorption of the selected target species as well as the kinetic and thermodynamic properties must be characterized. Therefore, a full characterization of the material was performed to determine the kinetics, isotherms and sorption profiles of iron(III) as a function of pH. For the colorimetric iron(III) sensing behavior of the membrane, the membrane is initially colorless and transparent but after immersion in iron(III) solutions, it turns red within minutes. Its performance was evaluated using ultraviolet-visible spectroscopy (UV/vis). In addition, a titration curve was constructed using the UV/vis data from the spectra recorded from sensory discs placed in contact with water solutions containing different iron(III) concentrations. Moreover, the titration was also performed using an image of the sensory discs (i.e., color digital definition (RGB parameters) of the previously mentioned sensory discs (computer vision-based analytical chemistry). Therefore, the solid sensory discs are manageable materials that can be handle without care, stored under ambient conditions for long periods of time, and used to measure the concentration of Fe(III) even by untrained personnel using images recorded using widely available devices, such as mobile phones and tablets.

## **2. EXPERIMENTAL SECTION**

The materials, synthetic procedures and measurements methods and methodologies are described in the Supporting Information (ESI) in Section S1.

### **2.1. Preparation of sensory materials**

The sensory monomer derived from Kojic acid (**3**) was prepared according with the experimental procedure described in the ESI (Section S1) and shown schematically in Scheme 1.

The film-shaped sensory membranes were prepared via bulk radical polymerization of hydrophilic monomers including 1-vinyl-2-pyrrolidone (**VP**), 2-hydroxyethyl acrylate (**2HEA**), and a monomer derived from Kojic acid (**3**). Ethylene glycol dimethacrylate (**EGDMA**) was used as a cross-linking agent (Scheme 2). The **VP/2HEA/(3)/EGDMA** comonomer molar ratio was 75/24/1/10. AIBN (1 wt%) was employed as a thermal radical initiator. The bulk radical polymerization reaction was carried out in a 200  $\mu\text{m}$  thick silanized glass mold in an oxygen-free atmosphere at 60°C overnight. After demolding, the film was conditioned at 60°C for an additional night. The solid sensory substrates were manufactured from the film-shaped membrane by using a puncher to cut out sensory discs (8 mm diameter).

### Scheme 1.

### Scheme 2

## 3. RESULTS AND DISCUSSION

Our objective was to prepare an easily handled solid material for the extraction, detection and quantification of Fe(III) in pure water. The material consists a film-shaped polymer network with derivative of Kojic acid in its structure, which acts as a receptor and chemosensory core for Fe(III). The polymer has a cross-linked structure that is hydrophilic and acts as a membrane with gel behavior, allowing Fe(III) ions in water to enter into the material as solvated species where they interact with the receptors to give

rise to the extraction and sensing phenomena. Kojic acid was chosen as the receptor because it is a natural product and a well-known chelating ligand that strongly coordinates to iron(III), which results in red-colored complexes [14-16]. Moreover, Kojic acid has been used for many years for the spectrophotometric determination of iron in different contexts (e.g., in ores) [17,18]. Therefore, we designed and prepared an acrylic monomer (**3**) containing a Kojic acid sensory motif to synthesize a membrane for use as a colorimetric sensor and solid-phase extractant (Scheme 1). The mechanism of detection and extraction of Fe(III) involves the formation of red  $\text{Fe(III)}_n:(\text{Kojate motifs})_m$  chelates with primary stoichiometries (n:m) of 1:1, 1:2 and 1:3 (Scheme S1, ESI). The stability constants for the interaction between iron(III) and Kojic acid have been reported by Muraki and are  $\log K_1 = 10.20$ ,  $\log K_2 = 8.78$ , and  $\log K_3 = 7.53$  [16]. The stoichiometry of the  $\text{Fe(III)}_n:(\text{Kojate motifs})_m$  species in the solid state (i.e., inside the membrane) and the relative exchange coefficients that are described below for our system are in agreement with those for the species in solution [16].

### 3.1. Material preparation and characterization

The methacrylate sensory monomer (**3**) could not be conventionally prepared in a single step from Kojic acid and methacryloyl chloride but was synthesized using a two-step procedure. First, the treatment of Kojic acid with thionyl chloride led to the reaction of the primary alcohol with the formation of a Kojic acid primary chloro-derivative [19] that led to (**3**) by reaction with potassium methacrylate at 100°C (no thermal initiated polymerization was observed) [20]. The reaction steps are schematically shown in Scheme 1. The  $^1\text{H}$  and  $^{13}\text{C}$  NMR as well as FTIR spectra of the intermediates and monomers are provided in the experimental section and in the ESI, Section S1. The potential applicability of the sensory membrane was confirmed by the fact that less than

1.6% by weight of the sensory synthetic monomer (**3**) was used in the preparation of the sensory material and >98.4% by weight of commercial and inexpensive comonomers.

The membrane or film exhibits a good physical appearance and was creasable and easily handled. The thermal resistance was evaluated by thermogravimetric analysis (TGA). The degradation temperatures that resulted in a 5% and 10% weight loss under inert and oxidizing atmospheres ( $T_5$ ) were ~280°C and ~280°C, respectively, which is in agreement with the TGA data for the **VP** and **2HEA** copolymers [10,21]. The thermal degradation patterns were affected by the sorption of Fe(III) by the membrane. The immersion of the membrane in water containing a relatively low concentration of Fe(III) increased  $T_5$  to 355°C due to the additional crosslinking caused by the formation of Fe(III)<sub>1</sub>:(Kojic acid moieties)<sub>2</sub> and Fe(III)<sub>1</sub>:(Kojic acid moieties)<sub>3</sub> (Figure S5, ESI). In contrast, immersion in water with a higher concentration of Fe(III) decreased  $T_5$  to 300°C due to partial displacement or complexation to Fe(III)<sub>1</sub>:(Kojic acid moieties)<sub>1</sub> species with a concomitant decrease in the crosslinking density (please see the sorption and sensing results below).

Gel behavior is relevant for a membrane to sense in pure water because the target species enter into the material as solvated species by diffusion. However, the water uptake has to be modulated to maintained good mechanical properties in the swelled state. Therefore, a moderate water swelling percentage ranging from 40% to 100% is desirable. The membrane composition was designed to meet this criterion, and its water swelling percentage was 65%.

## **3.2. Sorption studies**

### **3.2.1. Sorption kinetics and isotherms**

For example, the kinetic profiles of iron(III) sorption on the membrane are shown in Figure 1. Kinetic experiments are useful to determine the time required to reach equilibrium between the two phases. The experiments were performed under acid conditions (pH 2.5) to avoid iron(III) hydrolysis reactions.

Iron(III) sorption on the membrane required approximately 30 min to achieve equilibrium. The experimental data are fitted using a HPDM model (homogeneous particle diffusion model) where the diffusion of ions from the solution to the sorbent is the slowest step. The relationship between the amount of sorbed metal ion in the solid phase ( $q$ , mmol g<sup>-1</sup>) and time ( $t$ , min) is formally equal to the pseudo first order kinetic equation [22], and the rate constant ( $k$ ) was determined to be 0.20(2) min<sup>-1</sup> ( $R^2=0.979$ ; SE(y) = 0.015).

### Figure 1.

The sorption isotherm of iron(III) on the membrane in a 0.1 M KNO<sub>3</sub> solution at 25°C and pH 2.5 are shown in Figure 2.

### Figure 2.

The Langmuir and Freundlich models are typically employed to describe the relationship between  $q$  (sorbed quantity in the solid phase, mmol g<sup>-1</sup>) and  $C_{eq}$  (solute concentration at equilibrium). Their varied performances have been previously reviewed [23].

The Langmuir model provided the best description of the sorption of Fe(III) on the membrane. Based on non-linear fitting of the data in Figure 2, the maximum sorption capacity  $q_{max}$  was 0.041(2) mmol g<sup>-1</sup>, and  $K_L = 6.5(9) \times 10^3$  M<sup>-1</sup> ( $R^2 = 0.984$ ;



SE(y) = 0.002). The theoretical total number of active sites calculated from the weight percentages of (3) in the membrane was 0.07 mmol g<sup>-1</sup>, which is in agreement with the obtained  $q_{\max}$ .

### 3.2.2. Sorption profiles

The thermodynamic characterization of ion-exchange and chelating materials is fundamental for describing the separation process and predicting the behavior of analyte sorption on solid phases in different systems. As previously mentioned, especially for ion-exchange and complexing resins [23-25], a metal ion (M) can be sorbed onto a chelating solid phase via complexation reactions, and the general equilibrium can be expressed as follows:



where M is the metal ion, H<sub>r</sub>L is the r-protonated form of the active site of the solid phase, H is the proton, and the overbar represents species in the solid phase. Charges are omitted for simplicity. This reaction is studied based on the sorption profiles as a function of pH. This method has been previously described in several papers and reviews [23-28]. This method enables us to describe the sorption curve with an equation obtained using a combination of exchange coefficients ( $\beta_{1npex}$ ) that are associated with each possible reaction between the metal ion and the active site and selected to minimize the difference between the calculated and experimental sorption profiles.

The exchange coefficient ( $\beta_{1npex}$ ) can be expressed as follows:

$$\beta_{1npex} = \frac{[\overline{MH_pL_n}] \cdot [H]^q}{[M] \cdot [\overline{H_rL}]^n} \quad (2)$$

The exchange coefficients depend on the concentration of the counter ion in the solution and in the solid phase, and the intrinsic complexation constants ( $\beta_{1npi}$ ) are independent of the composition of the solution. Therefore, these values characterize the sorption equilibria. The relationship between the exchange coefficient and the intrinsic complexation constant can be expressed as follows [23,24]:

$$\beta_{1npi} = \beta_{1npeX} \cdot \frac{\gamma_H^q \cdot \gamma_C^{(m-q)}}{\gamma_M} \cdot \frac{[C]^{(m-q)}}{[\bar{C}]^{(m-q)}} \quad (3)$$

where  $m$  is the charge of the metal,  $\gamma_X$  is the activity coefficients of species  $X$  and  $C$  is the counter ion of the active site of the solid material.

Different experiments were performed under different conditions, and the set of intrinsic constants that were calculated in the first experiment should be equal (within the experimental error) to that determined under any other studied conditions. The intrinsic protonation constants are independent of the experimental conditions. Therefore, these constants characterize the sorption reactions. For simplicity, the active sites in the solid phase are always in analytical excess with respect to the metal ion because these conditions are close to those in a practical application.

Once the reactions have been identified, the ligand properties of the solid phase in the considered ionic media and at the specific pH values can be described by a partition coefficient ( $K^*$ ), which represents the ratio of total metal ions in the solid phase to free metal ions in solution and can be expressed as follows:

$$K^* = \frac{c \cdot V}{[M] \cdot w} = \sum \frac{\beta_{1npeX} [\overline{H_r L}]^n}{[H]^q} \quad (4)$$

where  $c$  is the concentration of the sorbed metal,  $V$  (mL) is the volume of the solution phase and  $w$  (g) is the mass of dry solid material. The summation is extended to all of the complexes that are formed by the considered metal ion with the active group of the solid phase.

The strategy for selecting the sorption reactions begins by considering the simplest stoichiometries and reactions equal to those of the "monomeric units" in solution. In this study, we selected the complexation constants of the Fe(III)/Kojic acid complexes in aqueous solution as input data.

Some examples of the sorption profiles are shown in Figure 3, where the symbols represent the experimental data and the continuous lines represent the calculated sorption curves.

The sorption was studied both in the absence and presence of two different ligands (i.e., 2,6-pyridine dicarboxylic acid (PDCA) and sodium oxalate). These ligands compete with active sites on the membrane, shift the sorption at a higher pH, and make it possible to identify any other complexes of the metal ion with the solid phase.

### Figure 3.

A fairly good fit was obtained for all three profiles assuming the formation of the following complexes in solid phase with the same set of exchange coefficients:  $\text{FeL}$   $\log\beta_{101\text{ex}} = 10(5)$ ,  $\text{FeL}_2$   $\log\beta_{102\text{ex}} = 19.8(4)$ ,  $\text{FeL}_3$   $\log\beta_{103\text{ex}} \approx 25.3$ ,  $\text{FeHL}_3$   $\log\beta_{113\text{ex}} = 32.7(9)$ , and  $\text{Fe(OH)L}_3$   $\log\beta_{1-13\text{ex}} = 17.5(3)$ . The first three exchange coefficients in the solid phase are in good agreement with the computed conditional constants in solution [16].

Based on these results, two other protonated species (i.e.,  $\text{FeHL}_3$  and  $\text{FeL}_3\text{OH}$ ) can be formed in the solid phase. These complexes have never been previously reported for Kojic acid in aqueous solutions but they are most likely promoted by the high concentration of active groups inside the membrane. We have confirmed the formation of these apparently unusual complexes in different cases with commercial chelating resins and different metal ions [24,29-32].

### **3.3. Sensing Fe(III) in aqueous media**

#### ***3.3.1 Detection and quantification of Fe(III) in water***

The immersion of the sensory discs that were cut from the sensory membrane in water containing Fe(III) resulted in the discs changing color from colorless to red, and the color development as a function of the Fe(III) concentration.

Therefore, a Fe(III) titration curve was constructed using a set of 7 sensory discs after immersion overnight in Milli-Q water containing different concentrations of Fe(III) (i.e., ranging from  $1.65 \times 10^{-6}$  to  $1.65 \times 10^{-1}$  M) under acidic conditions (pH = 2, HCl/KCl buffer). A control sensory disc that was immersed in this medium in the absence of Fe(III) was also prepared. Then, the discs were removed from the aqueous solution and allowed to dry under ambient conditions. The color development within the discs as the concentration of Fe(III) increased was visible and permitted the semi-quantitative naked eye titration of Fe(III), and their UV/vis spectra allowed for the construction of a titration curve (Figures 4a and 4b). The limits of detection and quantification were  $3.6 \times 10^{-5}$  and  $1.1 \times 10^{-4}$  M, respectively.

Increasing attention has been focused on chemical analysis based on color changes recorded with ubiquitous imaging devices to develop user-friendly analytical

procedures for in situ and real-time monitoring [33]. Therefore, digital images of the discs were recorded to construct a titration curve using the digital color definition (RGB parameters) of the sensory discs (Figure 4c; Section S4, ESI) [10,34]. The limits of detection and quantification were  $2.0 \times 10^{-5}$  and  $6.0 \times 10^{-5}$  M, respectively. To determine the applicability of the sensory material to real samples, a test sample containing a Fe(III) concentration of  $3.31 \times 10^{-4}$  M was prepared using tap water that was buffered at a pH of 2 (the concentration of Fe(III) corresponded to the sum of the added and innate tap water ferric ion concentration). The calibration curves that were obtained using the UV/vis spectra and digital pictures (RGB parameters) of the reference discs immersed in tap water (buffered at pH = 2; concentration ranging from  $1.0 \times 10^{-5}$  to  $1.0 \times 10^{-3}$  M) allowed for the calculation of the concentration of the test sample, which was in agreement with the real value (calculated concentration using UV/vis and RGB parameters of digital images:  $3.26 \times 10^{-4}$  and  $3.29 \times 10^{-4}$  M, respectively).

The limit of detection is relatively high and higher than the US National Secondary Drinking Water Regulations for iron (0.3 mg/L,  $5.4 \times 10^{-6}$  M) as well as that reported by Gupta et al. ( $1.9 \times 10^{-8}$  M [2];  $9.5 \times 10^{-7}$  M [3];  $5.0 \times 10^{-6}$  M [8]) and ourselves ( $2.5 \times 10^{-6}$  M [10],  $1.3 \times 10^{-7}$  [13]). However, the response of the sensory material could be tuned by modifying the molar ratio of the monomers used in the synthesis of the sensory membrane. For example, the response could be improved by increasing the molar ratio of iron receptors (Kojic acid derivative monomer (**3**)).

#### Figure 4.

### 3.3.2. Response time

The response time is a key parameter for sensor performance in real-life applications. Therefore, the response time of the membrane immersed in solution was investigated using UV/vis spectroscopy to determine the time required to achieve 99% of the absorbance (490 nm) variation (Figure 5). This time was 20 min for a water solution containing an Fe(III) concentration of  $5 \times 10^{-3}$  M. This time accounts for the diffusion of the species into the membrane and concomitant reaction with the Kojic acid motifs. This time is in agreement with the time required to reach equilibrium between the two phases, which was previously analyzed to describe the sorption kinetics.

### Figure 5.

#### 3.3.3. Interference study

The selectivity study was initially carried out according to a previous preparation method for the sensory material using a  $1.6 \times 10^{-3}$  M solution of monomer (**3**) in DMA/H<sub>2</sub>O (50/50). To this solution, a solution containing a broad set of cations and anions (see Figures S6 and S7, ESI) were added ( $1.6 \times 10^{-2}$  M for each species). Red color development was observed for Fe(III), and the system did not exhibit a response to the other cations and anions (Figure 6 shows the UV/vis response to the cations and Figure S7, ESI, show the UV/vis response to the anions). This selectivity of the solid sensory membrane was confirmed both visually and by a computer vision-based analysis, e.g., the sensory discs yielded the same response for Fe(III) and a mixture of cations (Figure 6).

### Figure 6.

## Figure 7.

### 4. CONCLUSIONS

We used Kojic acid, which is a natural chelating agent for iron(III), to prepare a colorimetric sensory polymer as a solid film (membrane). The Kojic acid derivative, which is chemically anchored to the polymer backbone, acted as an excellent receptor for Fe(III) in water media. The characterization of the sorption of Fe(III) on the membrane indicated that the sorption followed pseudo first order kinetics, and the sorption required approximately 30 min to reach equilibrium. The sorption isotherms are well modeled using the Langmuir equation, and the maximum sorption capacity was approximately 0.04 mmol/g. The complexes that were found in the solid phase are in good agreement with those previously identified in the aqueous phase. Colorless discs that were cut from the sensor membrane (8 mm diameter) for use as solid titration kits turned red upon contact with water solutions containing Fe(III). The color development permitted both visual concentration estimation using the naked eye and titration using the UV/vis technique. The limit of detection for Fe(III) was  $3.6 \times 10^{-5}$  M with a dynamic range determination of five decades (lower concentration =  $1.65 \times 10^{-6}$  M). In addition, images of the kits permitted titration using the color definition of the sensory discs as analytical input (limit of detection of  $2.0 \times 10^{-5}$  M). Therefore, the color development of the sensory system and the practical solid kits enabled the visual use of these materials by everyone regardless of their background. In addition, portable devices, such as

tablets and smartphones, allow for out-of-lab quantification of target species in an in situ, rapid and inexpensive fashion.

### Acknowledgments

We gratefully acknowledge the financial support provided by FAR (Fondi Ateneo per la Ricerca) of the University of Pavia, by the Spanish Ministerio de Economía y Competitividad-Feder (MAT2014-54137-R) and by the Consejería de Educación – Junta de Castilla y León (BU232U13).

### Supporting information

Experimental (intermediates and membrane characterization) and principal component analysis (PCA) data.

### References and notes

- [1] H. G. Seiler, A. Sigel, H. Sigel, Handbook on Metals in Clinical and Analytical Chemistry, Marcel Dekker, Inc., NY, 1994, p.13.
- [2] V. K. Gupta, N. Mergu, L. K. Kumawat, A new multifunctional rhodamine-derived probe for colorimetric sensing of Cu(II) and Al(III) and fluorometric sensing of Fe(III) in aqueous media, Sens. Actuators B 223 (2016) 101-113.
- [3] V. K. Gupta, A. K. Singh, L. K. Kumawat, N. Mergu, An easily accessible switch-on optical chemosensor for the detection of noxious metal ions Ni(II), Zn(II), Fe(III) and UO<sub>2</sub>(II), Sens. Actuators B 222 (2016) 468-482.
- [4] V. K. Gupta, N. Mergu, A. K. Singh, Rhodamine-derived highly sensitive and selective colorimetric and off-on optical chemosensors for Cr<sup>3+</sup>, Sens. Actuators B 220 (2015) 420-432.
- [5] V. K. Gupta, B. Sethi, N. Upadhyay, S. Kumar, R. Singh, L. Pratap Singh, Iron (III) Selective Electrode Based on *S*-Methyl *N*-(Methylcarbamoyloxy) Thioacetimidate as a Sensing Material, Int. J. Electrochem. Sci. 6 (2011) 650-663.
- [6] M. Kumar, L. K. Kumawat, V. K. Gupta, A. Sharma, 2-(Alkylamino)-3-aryl-6,7-dihydrobenzofuran-4(5*H*)-ones: Improved Synthesis and their Photophysical Properties, ChemistryOpen 4 (2015) 626-632.
- [7] V. K. Gupta, A. K. Singh, L. K. Kumawat, Thiazole Schiff base turn-on fluorescent chemosensor for Al<sup>3+</sup> ion, Sens. Actuators B 195 (2014) 98-108.
- [8] V. K. Gupta, A. K. Jain, S. Agarwal, G. Maheshwari, An iron(III) ion-selective sensor based on a  $\mu$ -bis(tridentate) ligand, Talanta 71 (2007) 1964-1968.
- [9] F. G. Banica, Chemical Sensors and Biosensors: fundamentals and applications, Wiley, Chichester, 2012, p. 576.
- [10] S. Vallejos, A. Munoz, S. Ibeas, F. Serna, F. C. García, J. M. García, Solid sensory polymer substrates for the quantification of iron in blood, wine and water by a scalable RGB technique, J. Mater. Chem. A 1 (2013) 15435-15441.



- [11] R. Biesuz, G. Emma, C. Milanese, G. Dacarro, A. Taglietti, V. M. Nurchi, G. Alberti, Novel DFO-SAM on mesoporous silica for iron sensing. Part I. Synthesis optimization and characterization of the material, *Analyst* 139 (2014) 3932-3939.
- [12] G. Alberti, G. Emma, R. Colleoni, M. Pesavento, V. M. Nurchi, R. Biesuz, Novel DFO-functionalized mesoporous silica for iron sensing. Part 2. Experimental detection of free iron concentration (pFe) in urine samples, *Analyst* 139 (2014) 3940-3948.
- [13] M. Trigo-López, A. Muñoz, S. Ibeas, F. Serna, F. C. García, J. M. García, Colorimetric detection and determination of Fe(III), Co(II), Cu(II) and Sn(II) in aqueous media by acrylic polymers with pendant terpyridine motifs, *Sens. Actuators B* 226 (2016) 118–126.
- [14] M. Zirak, B. Eftekhari-Sis, Kojic acid in organic synthesis, *Turk. J. Chem.* 39 (2015) 439-496.
- [15] V. M. Nurchi, J. I. Lachowicz, G. Crisponi, S. Murgia, M. Arca, A. Pintus, P. Gans, J. Niclos-Gutierrez, A. Domínguez-Martín, A. Castineiras, M. Remelli, Z. Szewczuk, T. Lis, Kojic acid derivatives as powerful chelators for iron(III) and aluminium(III), *Dalton Trans.* 40 (2011) 5984-5998.
- [16] Y. Murakami, Complexing behaviour of kojic acid with metal ions-II: Fe(III) chelates, *J. Inorg. Nucl. Chem.*, 24 (1962) 679-688.
- [17] M. L. Moss, M. G. Mellon, Colorimetric Determination of Iron with Kojic Acid, *Ind. Eng. Chem.* 13 (1941) 612-614.
- [18] J. P. Mehlig, M. J. Shepherd Jr., Spectrophotometric Determination of Iron in Ores with Kojic Acid, *Anal. Chem.* 21 (1949) 642-643.
- [19] S. M. Meier, M. Novak, W. Kandioller, M. A. Jakupec, V. B. Arion, N. Metzler, B. K. Keppler, C. G. Hartinger, Identification of the Structural Determinants for Anticancer Activity of a Ruthenium Arene Peptide Conjugate, *Chem. Eur. J.* 19 (2013) 9297-9307.
- [20] J-C. Cho, H. S. Rho, Y. H. Joo, C. S. Lee, J. Lee, S. M. Ahn, J. E. Kim, S. S. Shin, Y-H. Park, K-D. Suh, S. N. Park, Depigmenting activities of kojic acid derivatives without tyrosinase inhibitory activities, *Bioorg. Med. Chem. Lett.* 2012, 22, 4159-4162.
- [21] B. Redondo-Foj, M. Carsi, P. Ortiz-Serna, M. J. Sanchís, S. Vallejos, F. García, J. M. García, Effect of the Dipole–Dipole Interactions in the Molecular Dynamics of Poly(vinylpyrrolidone)-Based Copolymers, *Macromolecules* 47 (2014) 5334-5346.
- [22] H. Yuh-Shan, Citation review of Lagergren kinetic rate equation on absorption reactions, *Scientometrics* 59 (2004) 171-177.
- [23] G. Alberti, V. Amendola, M. Pesavento, R. Biesuz, Beyond the synthesis of novel solid phases: Review on modelling of sorption phenomena, *Coord. Chem. Rev.* 256 (2012) 28-45.
- [24] G. Alberti, M. Pesavento, R. Biesuz, A chelating resin as a probe for the copper(II) distribution in grape wines, *React. Funct. Polym.* 67 (2007) 1083-1093.
- [25] M. Pesavento, R. Biesuz, G. Alberti, M. Sturini, Characterization of the sorption of uranium(VI) on different complexing resins, *Anal. Bioanal. Chem.* 376 (2003) 1023-1029.
- [26] G. Alberti, R. Biesuz, A. Profumo, M. Pesavento, Determination of the total concentration and speciation of Al(III) in tea infusions, *J. Inorg. Biochem.* 97 (2003) 79-88.
- [27] G. Alberti, R. Biesuz, and M. Pesavento, Determination of the total concentration and speciation of Uranium in natural waters by the Resin Titration method, *Microchem. J.* 86 (2007) 166-173
- [28] G. Alberti, M.G. Guiso, and R. Biesuz, Usage of Empore (TM) membrane in alcoholic media for copper(II) distribution studies, *Talanta* 79 (2009) 603-612.
- [29] M. Pesavento, R. Biesuz, J.L. Cortina, Sorption of metal-ions on a weak acid cation-exchange resin containing carboxylic groups, *Anal. Chim. Acta* 298 (1994) 225-232.
- [30] M. Pesavento, R. Biesuz, Sorption of divalent metal ions on an iminodiacetic resin from artificial seawater, *Anal. Chim. Acta* 346 (1997) 381-391.
- [31] R. Biesuz, M. Pesavento, G. Alberti, F. Dalla Riva, Investigation on sorption equilibria of Mn(II), Cu(II) and Cd(II) on a carboxylic resin by the Gibbs – Donnan model, *Talanta* 5 (2001) 541-550.
- [32] R. Biesuz, G. Alberti, M. Pesavento, Sorption of lead(II) on two chelating resins: from the exchange coefficient to the intrinsic complexation constant, *J. Solution Chem.* 37 (2008) 527-541.
- [33] L. F. Capitan-Vallvey, N. López-Ruiz, A. Martínez-Olmos, M. M. Erenas, A. J. Palma, Recent developments in computer vision-based analytical chemistry: A tutorial review, *Anal. Chim. Acta* 899 (2015) 23-56.

- [34] H. El Kaoutit, P. Estevez, F. C. García, F. Serna, J. M. García, Sub-ppm quantification of Hg(II) in aqueous media using both the naked eye and digital information from pictures of a colorimetric sensory polymer membrane taken with the digital camera of a conventional mobile phone, *Anal. Methods* 5 (2013) 54-58.

## FIGURES AND SCHEMES

### Captions

**Scheme 1.** Synthesis of acrylic monomer (**2**).

**Scheme 2.** Monomers and chemical structure of the sensory membrane. The picture shows the physical aspect of the membrane on a notebook.

**Figure 3.** Sorption profiles of Fe(III) on 26.5 mg of dry membrane in 1 M KNO<sub>3</sub>, V = 10 mL, [Fe(III)] = 1.8 μM. Red circles = profile in absence of competitive ligand, blue diamonds = profile in presence of pyridine dicarboxylic acid (PDCA) 0.5 mM, green circles = profile in presence of sodium oxalate 0.05 M.

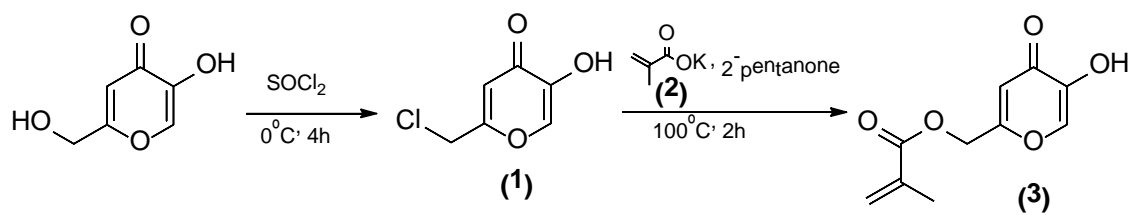
**Figure 2.** Sorption isotherm of Fe(III) on the membrane (sorbed metal ion in the solid phase (*q*) as a function of the solute concentration when the equilibrium is reached (*C<sub>eq</sub>*). Conditions: volume = 10 mL 0.1 M KNO<sub>3</sub>, pH 2.5, temperature = 25°C, 36.5 mg of dry membrane. Gray circles: experimental points; continuous line: best fitting by Langmuir model.

**Figure 1.** Kinetic profile of Fe(III) uptake on the membrane (sorbed metal ion in the solid phase (*q*) as a function of time (*t*)). Conditions: volume = 10 mL 0.1 M KNO<sub>3</sub>, pH = 2.5, temperature = 25°C, [Fe(III)] = 1.34 · 10<sup>-4</sup> M, 13.7 mg of dry membrane. The lines represent the fit obtained using a pseudo first order equation.

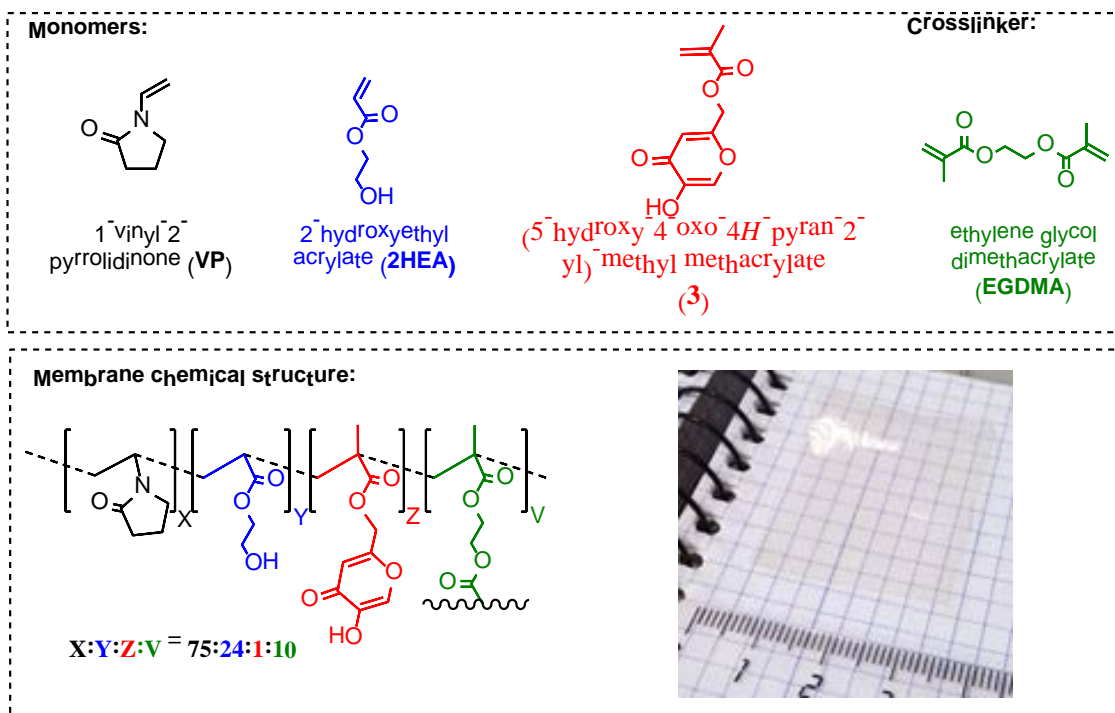
**Figure 4.** Colorimetric determination of the Fe(III) concentration in water using sensory discs cut from the membrane: a) UV/vis spectra (inset: picture of the discs, left disc is control disc); b) UV/vis titration curve; c) titration using the RGB parameters from the digital image taken from the sensory materials (see inset, Figure 5a). The three parameters (R, G and B) defining the color of each disc were reduced to one principal component (PC1) by principal component analysis. Conditions: prior to each measurement, each disc was immersed overnight in Milli-Q water (temperature = 25°C, pH = 2 -buffer HCl/KCl-) containing a Fe(III) concentration ranging from 1.65x10<sup>-6</sup> to 1.65 x10<sup>-1</sup> M and then removed from the medium and dried at rt.

**Figure 5.** Response time. Selected UV/vis spectra as a function of the time that a piece of membrane (discs, 8 mm diameter) was immersed in water (pH = 2, buffer: KCl-HCl, 2 mL) in a UV/vis quartz cuvette upon addition of Fe(III) (concentration = 5x10<sup>-3</sup> M). Inset = Absorbance (490 nm) as a function of time.

**Figure 6.** Interference study. a) UV/vis absorbance variation at 483 nm for (**3**) in solution (DMAc/H<sub>2</sub>O, 50/50; pH = 2, buffer: KCl-HCl, 2 mL; [(**3**)] = 1.6x10<sup>-3</sup> M) after addition of various cations. Each cation was added individually in a (**3**)/cation molar ratio of 1/10 (the concentration of each cation was 1.6x10<sup>-2</sup> M). Inset: sample UV/vis spectra of solution (**3**) after addition of various cations (i.e., Fe(III), Co(II) and Hg(II)); and b) picture of two sensory discs after immersion overnight in water (pH = 2, buffer: KCl-HCl, 2 mL) containing Fe(III) ([Fe(III)] = 1 x 10<sup>-2</sup> M) and two mixtures of cations (the concentration of each cation was 1 x 10<sup>-2</sup> M).



**Scheme 1.** Synthesis of acrylic monomer (3).



**Scheme 2.** Monomers and chemical structure of the sensory membrane. The picture shows the physical aspect of the membrane on a notebook.

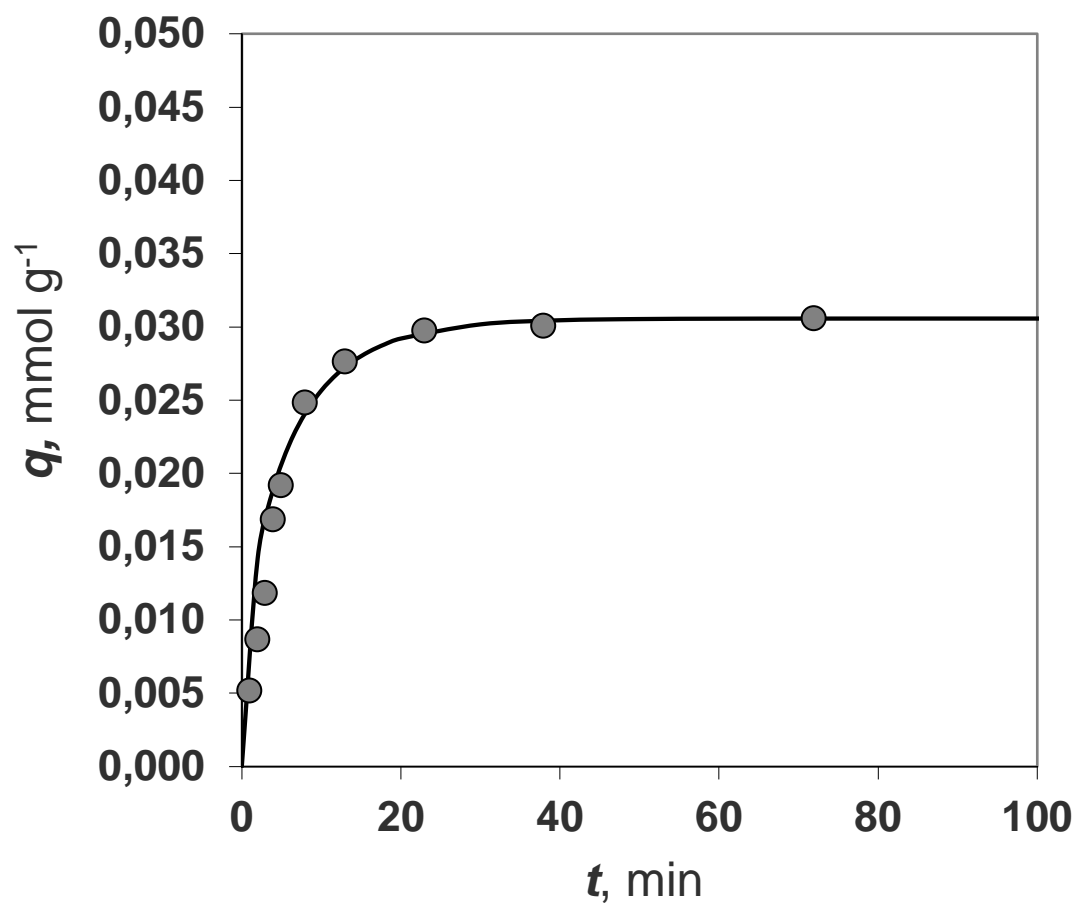


**Figure 1.** Kinetic profile of Fe(III) uptake on the membrane (sorbed metal ion in the solid phase ( $q$ ) as a function of time ( $t$ )). Conditions: volume = 10 mL 0.1 M  $\text{KNO}_3$ , pH = 2.5, temperature = 25°C,  $[\text{Fe(III)}] = 1.34 \cdot 10^{-4}$  M, 13.7 mg of dry membrane. The lines represent the fit obtained using a pseudo first order equation.

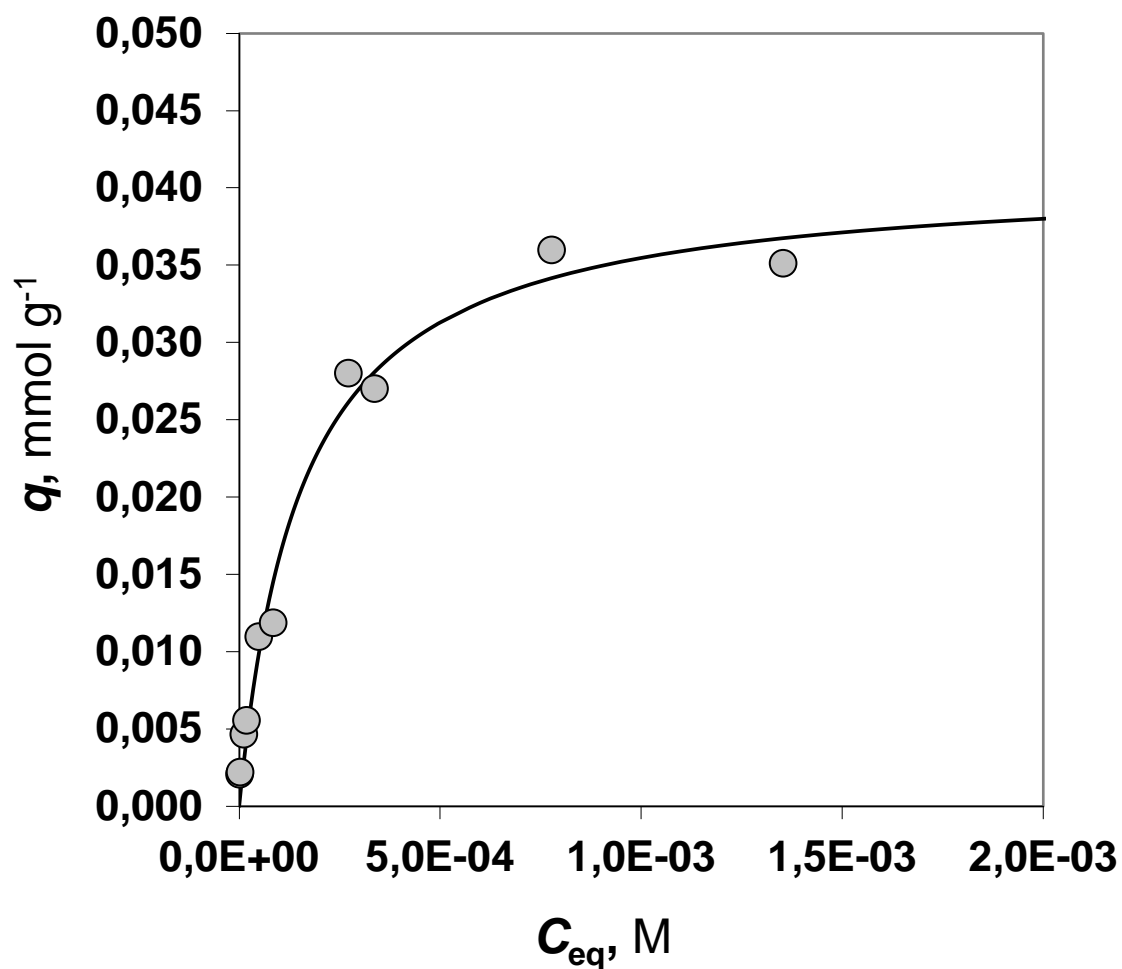


**Figure 2.** Sorption isotherm of Fe(III) on the membrane (sorbed metal ion in the solid phase ( $q$ ) as a function of the solute concentration when equilibrium is reached ( $C_{eq}$ )). Conditions: volume = 10 mL 0.1 M KNO<sub>3</sub>, pH 2.5, temperature = 25°C, 36.5 mg of dry membrane. Gray circles: experimental points; continuous line: best fitting by Langmuir model.

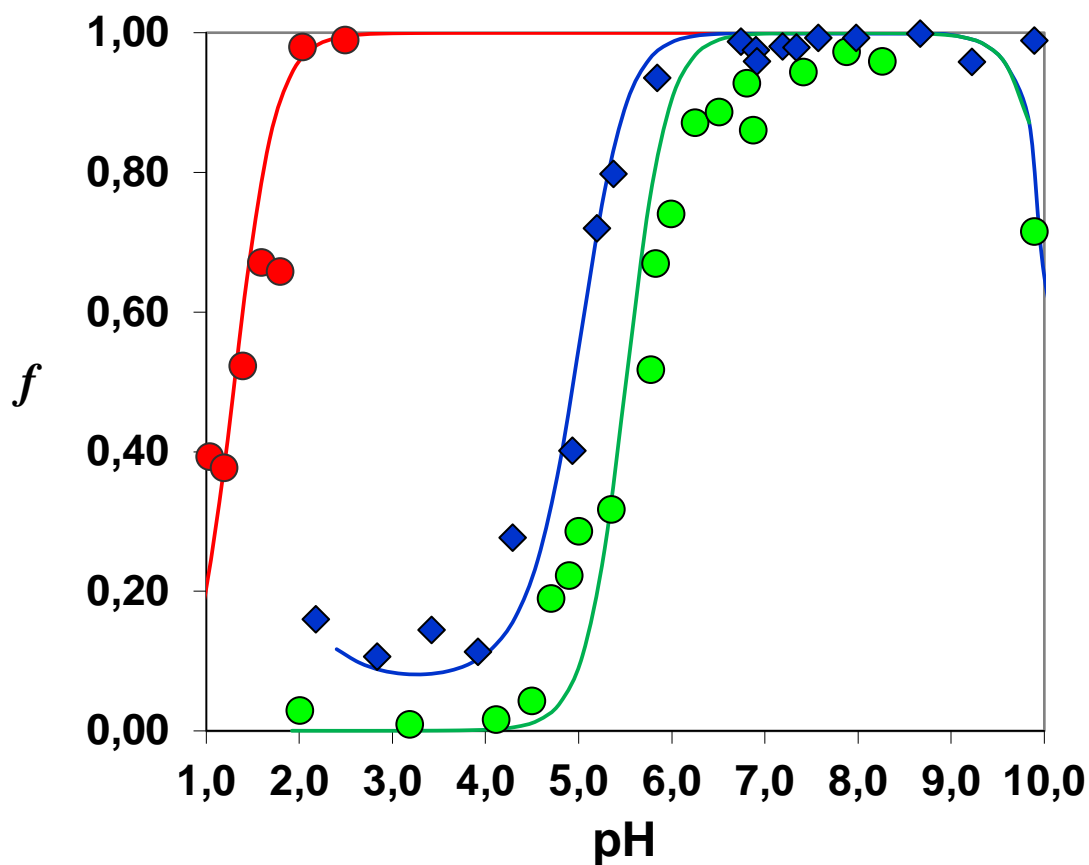


**Figure 3.** Sorption profiles of Fe(III) on 26.5 mg of dry membrane in 1 M KNO<sub>3</sub>, V = 10 mL, [Fe(III)] = 1.8 μM. Red circles = profile in absence of competitive ligand, blue diamonds = profile in presence of pyridine dicarboxylic acid (PDCA) 0.5 mM, green circles = profile in presence of sodium oxalate 0.05 M.



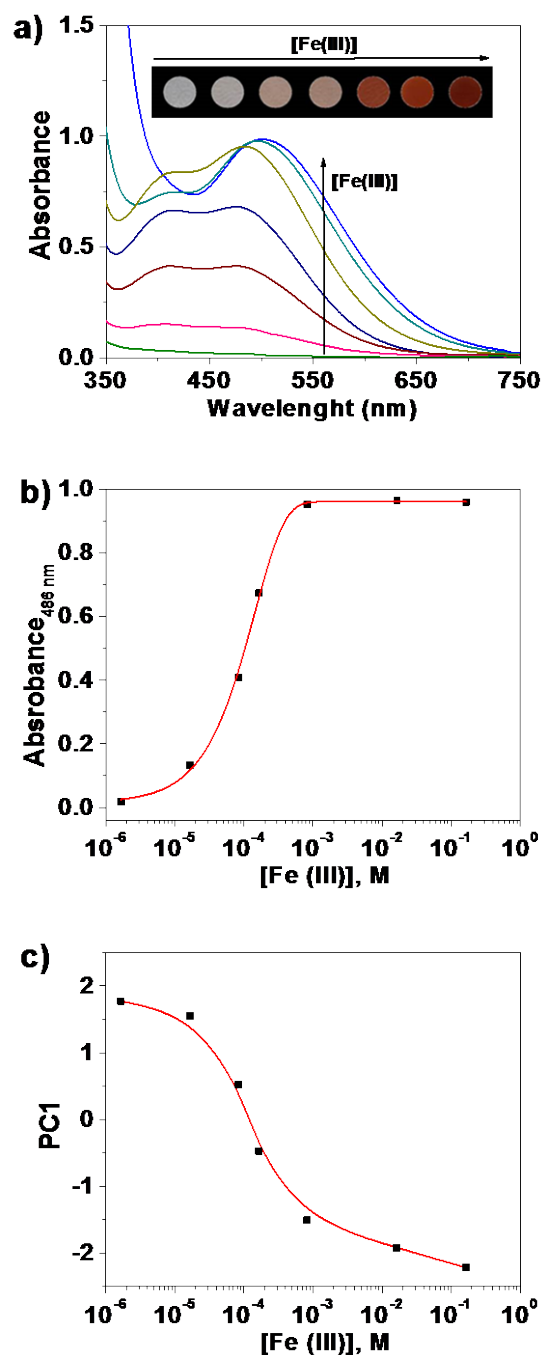


**Figure 4.** Colorimetric determination of the Fe(III) concentration in water using sensory discs cut from the membrane: a) UV/vis spectra (inset: picture of the discs, left disc is control disc); b) UV/vis titration curve; c) titration using the RGB parameters from the digital image taken from the sensory materials (see inset, Figure 5a). The three parameters (R, G and B) defining the color of each disc were reduced to one principal component (PC1) by principal component analysis. Conditions: prior to each measurement, each disc was immersed overnight in Milli-Q water (temperature = 25°C, pH = 2 -buffer HCl/KCl-) containing a Fe(III) concentration ranging from  $1.65 \times 10^{-6}$  to  $1.65 \times 10^{-1}$  M and then removed from the medium and dried at rt.

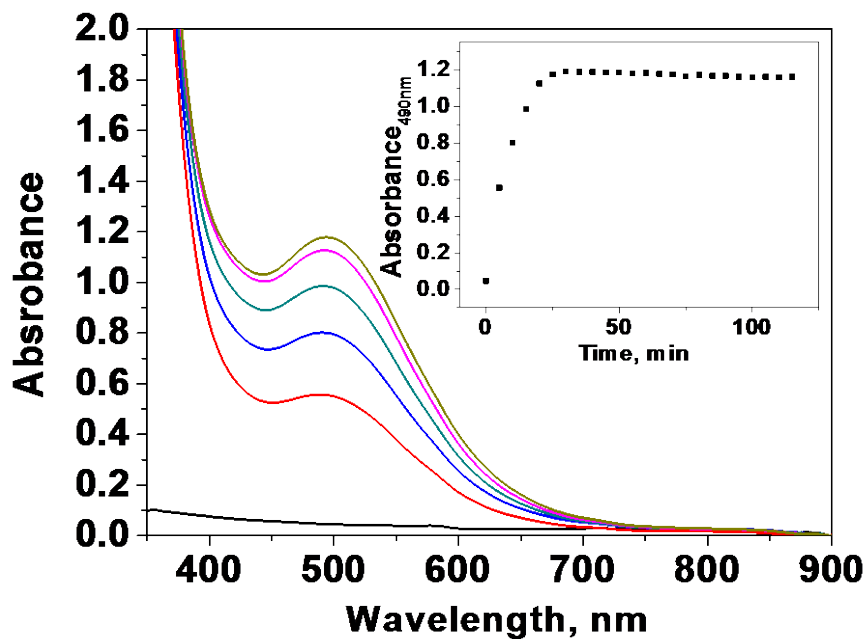


**Figure 5.** Response time. Selected UV/vis spectra as a function of the time that a piece of membrane (discs, 8 mm diameter) was immersed in water (pH = 2, buffer: KCl-HCl, 2 mL) in a UV/vis quartz cuvette upon addition of Fe(III) (concentration =  $5 \times 10^{-3}$  M). Inset = Absorbance (490 nm) as a function of time.

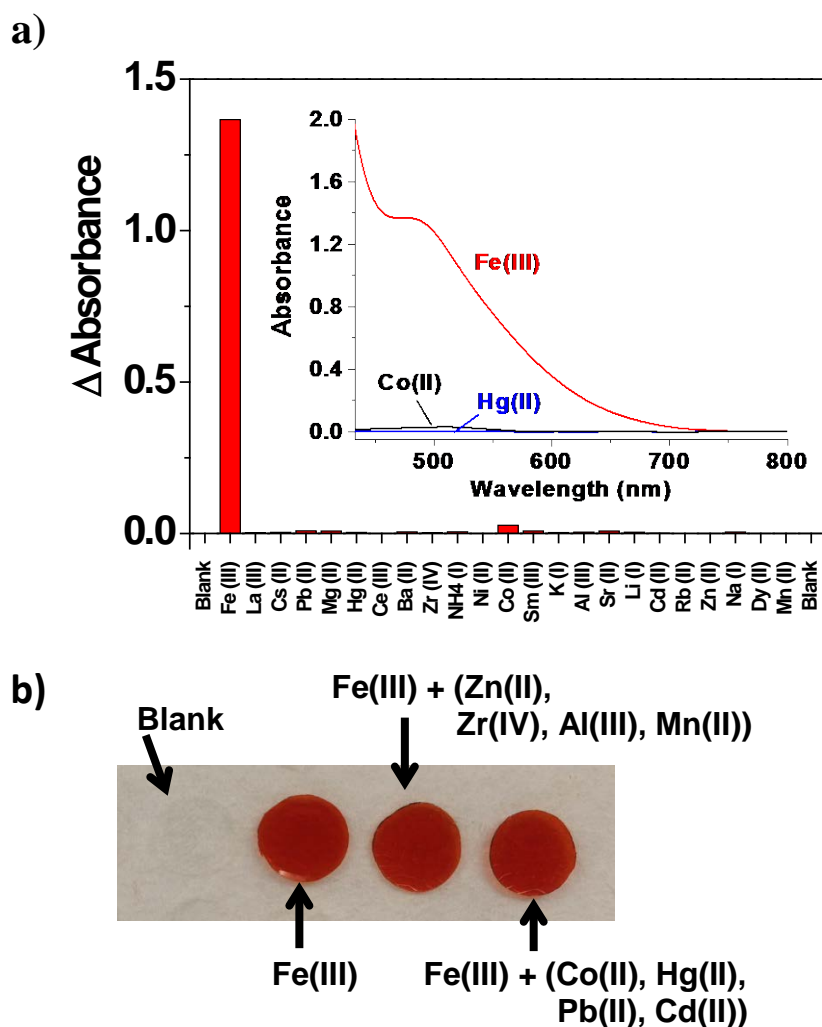


**Figure 6.** Interference study (cations). a) UV/vis absorbance variation at 483 nm of **(3)** in solution (DMAc/H<sub>2</sub>O, 50/50; pH = 2, buffer: KCl-HCl, 2 mL; [**(3)**] =  $1.6 \times 10^{-3}$  M) after addition of various cations. Each cation was added individually in a **(3)**/cation molar ratio of 1/10 (the concentration of each cation was  $1.6 \times 10^{-2}$  M). Inset: sample UV/vis spectra of solution **(3)** after addition of various cations (i.e., Fe(III), Co(II) and Hg(II)); and b) picture of two sensory discs after immersion overnight in water (pH = 2, buffer: KCl-HCl, 2 mL) containing Fe(III) ( $[\text{Fe(III)}] = 1 \times 10^{-2}$  M) and in two mixtures of cations (the concentration of each cation was  $1 \times 10^{-2}$  M).